Theoretical and experimental investigations on the threshold of a laser-induced breakdown of air

Dong Liu (刘 栋), Chuansong Chen (陈传松), Baoyuan Man (满宝元)*, Yanna Sun (孙艳娜), and Feifei Li (李菲菲)

School of Physics and Electronics, Shandong Normal University, Jinan 250014, China
**Corresponding author: byman@sdnu.edu.cn*

Received November 21, 2015; accepted February 23, 2016; posted online March 31, 2016

The threshold of a laser-induced breakdown of air is determined experimentally and theoretically. We find that the ionization of air has two steps: the first step is a multi-photon ionization process, which provides enough "seed electrons" to initiate the next step, and the second one is predominated by cascade ionization, which continues to produce free electrons geometrically until the critical free-electron density for breakdown is reached. So a two-step model based on the Morgan ionization model is established to describe the breakdown process. It is found that the time node dividing the two steps is about 9.8 ns in atmospheric air, and the threshold derived from the two-step model proposed here is more consistent with the experimental results than traditional ionization model.

OCIS codes: 020.0020, 020.2070, 020.4180.
doi: 10.3788/COL201614.040202.

An air breakdown and plasma formation will occur when a powerful laser pulse is focused on a very small region in air. The mechanisms of a laser-induced air breakdown have been investigated by many researchers in theory and experimentally since 1963[1]. It is greatly significant to study the mechanisms and thresholds for many fields, such as laser-induced lightning, laser ultra-wide-band radar, x ray laser production, laser-induced nuclear fusion, laser propulsion, and laser stealth. The laser-induced air plasma can generate intense terahertz waves that can serve as broadband terahertz sources[2]. In addition, the breakdown of ambient air must be considered carefully with laser-induced breakdown spectroscopy, which is a widely applicable analysis technology for determining compositions that are applied in atmospheric conditions[3–7]. Some researchers analyzed the laser-induced breakdown threshold of high-pressure water droplets to determine the number density of an aerosol in diesel engines; previously, there was no direct method to measure this[8]. Morgan investigated the ultraviolet, visible, and near-infrared laser-induced breakdowns and the process of plasma formation in gases[9]. He discussed the important roles of several ionization processes, such as multi-photon ionization (MI) and cascade collisional ionization in gas breakdowns, and proposed a model to describe the rate of change of the electron concentration caused by the combination of MI and cascade ionization (CI) processes. Gamal and Harith considered the MI and CI processes simultaneously under the influence of lasers with different wavelengths (0.693, 1.06, and 0.53 μm) and pulse durations (18, 7, and 25 ps)[10]. They calculated the threshold using the Runge–Kutta fourth-order method to solve the equation given by Ireland and Grey Morgan[11]. The calculated threshold is associated with avalanche breakdowns rather than MI.

Some researchers also studied the laser-induced breakdown process in air experimentally, and calculated the threshold based on the theories of MI and CI[12–18]. It is stated that the two processes play different roles with different kinds of gas, pressure, wavelength, and laser intensity. The MI will occur when the pulse intensity exceeds 10^{10} W/cm^2, and plays a more important part with the decrease of the wavelength[1]. The CI is the dominant mechanism when the pulse width exceeds 1 ps[14], but the cascade process can be initiated only if enough initial free electrons are produced. These initial electrons also called "seed electrons"; these first gain energy from laser pulses through inverse bremsstrahlung ionizing the neutrals by collisions. The generated electrons continue to absorb energy from the laser field and lead to the number of electrons increasing exponentially by electron-neutral collisions. However, there are not enough free electrons in the air to cause cascade breakdown under atmospheric pressure, so the "seed electrons" need to be generated by MI[18–20]. So far, most previous theoretical calculations have been performed based on the simultaneous effects of the MI and CI just by solving the equation of the non-linear ionization of gas. Nevertheless, some researchers divided the breakdown process into two equilong steps[14,20]. This kind of division is rough because the durations of the two steps may not be equal. Therefore, in order to gain insight into the whole process, the time node between the MI and CI steps needs to be determined accurately. In this work, we suggest that the breakdown occurs in two steps:

(1) The MI process produces the free electrons until the critical "seed electron" density n_{e0} is reached;
(2) Then, the "seed electrons" initiate the CI process, which generates free electrons much faster than MI

and rapidly becomes the dominant mechanism for ionization. This cascade-dominant step will continue until the breakdown criterion is satisfied.

Based on this two-step model, the threshold of the breakdown is determined and discussed in comparison with experimental and traditional models.

The experimental setup was schematically shown in our previous Letter[21–24]. A Q-switched Nd-YAG laser produces a near-infrared Gaussian laser pulse with a wavelength of 1064 nm and a pulse duration of 10 ns. The laser energy varies between 0 to 1 J/pulse and can be measured by a digital power meter (OPHIR DGX-30A). The laser beam is focused in air through a quartz lens with a focal length of 6.5 cm. The laser-induced air plasma forms in a closed chamber, which is used to keep a stable and adjustable ambient pressure in it and avoid the air flowing in the lab and thus disturbing the formation of the plasma. The plasma can be observed clearly through a circular window on the chamber.

The threshold of air breakdown at a given pressure is measured in the following manner. First, the chamber is filled with air up to the desired pressure. Then, the laser is fired and its power is increased until the gas breakdown is observed. The breakdown is easily determined because it is associated with a cracking noise and the appearance of a bright flash in the focal region. The breakdown becomes a sporadic event when the threshold is just reached[25]. The threshold for breakdown is taken to be the intensity that produces visible flashes of 30–50 of the laser shots[8,13,18,26]. We repeat the experiment 10 times under the same conditions and then average the results.

The phenomenon of the laser-induced breakdown of air is a complex simultaneous effect of several physical processes such as MI and CI, recombination of ions and electrons, and the diffusion of electrons. The latter two are considered to be the dominant electron-consuming mechanisms that reduce free electrons at the rate of 10^8/s[27]. In our experiment, the laser pulse duration is only 10 ns, so the consumption of the electrons is negligible during such a short time.

The production of the free electrons is dominated by two main mechanisms: MI and CI. The former refers to the process in which the neutrals absorb more than one laser photon simultaneously and valence electrons transit directly from the bound state to the free state. The latter refers to the process in which the free electrons ionize the neutral gas by frequently colliding with them, and this process produces more free electrons. The "new" electrons repeat the process above and the avalanche effect takes place.

The equation describing the rate of the electron density growth due to both the effects of MI and CI established by Ireland and Grey Morgan[11] is as follows:

$$\frac{\mathrm{d}n_e}{\mathrm{d}t} = n_e N(377\frac{q}{\omega^2}\left(\frac{v_m}{N}\right)^2 I(t) + \frac{NA}{k^{3/2}} I^k(t), \qquad (1)$$

where N is the neutral atoms' density in gas, q is the constant of a particular gas (typically of the order of 10^{21} cm^{-1} s^{-1} V^{-2}), $I(t)$ is the power density of the laser, ω is the angular frequency of the laser radiation, A is the absorption coefficient of the MI, and k is the number of the laser photons the MI needs[9]. The first term of Eq. (1) stands for the CI process, while the latter one indicates the MI process. Traditionally, the integral of Eq. (1) over the laser pulse duration is considered as the final electron density $n_{e\text{-final}}$. When $n_{e\text{-final}}$ is beyond a critical value of $n_{e\text{-th}}$, the breakdown takes place[9,10,18]. This way, we can evaluate the breakdown threshold I_{th}.

However, the relative roles of the two ionization mechanisms are different under different conditions. Whether both of them would take place under the present experimental conditions is uncertain. Generally, the ionization probability of the MI and CI depends on the relationship between the electron quiver energy $\varepsilon_{\mathrm{osc}}$ and the ionization potential J. If $\varepsilon_{\mathrm{osc}} > J$, the probability of MI (ω_{MI}) will be larger than that of the CI process (ω_{CI}), and vice versa[28]. The electron quiver energy can be written as $\varepsilon_{\mathrm{osc}} = e^2E/4\ m\omega^2$ with $E^2 = 2I/n\varepsilon_0 c$, where E and ω indicate the electric field and the angular frequency of the incident laser, respectively. In addition, e and m refer to the electron charge and mass, respectively. In the expression of E, I indicates the power density of the incident laser, n is the refraction index, ε_0 is the permittivity, and c refers to the speed of light in a vacuum[29]. In the present case, $I = 10^{12} - 10^{13}$ W/cm^2, $\omega = 1.78 \times 10^{15}$ s^{-1}, so $\varepsilon_{\mathrm{osc}} = 10^{-2}\ - 10^{-1}$ eV, which is lower than the ionization potentials $J_{\mathrm{N}} = 14.53$ eV (nitrogen) and $J_{\mathrm{O}} = 13.62$ eV (oxygen). Thus, probability of the MI process occurring is much smaller than that of CI process.

The ionization rates for the two processes can be written as $n_e\omega_{\mathrm{CI}}$ (CI process) and $N\omega_{\mathrm{MI}}$ (MI process), where n_e and N refer to the densities of free electrons and neutral atoms in air, respectively[28]. There is a small amount of free electrons in air before the laser treatment. They are derived from the ionizations of the materials with low ionization potentials in air that are induced by cosmic rays and ultraviolet rays from the sun. The density of these free electrons is $n_{e\text{-ini}} \approx 10^3$ cm^{-3}[23,30]. The number density of neutral atoms in air is $N \approx 3.56 \times 10^{16}$ P cm^{-3}, where P is the air pressure (in Torr). Thus, $n_{e\text{-ini}} \ll N$ while $\omega_{\mathrm{CI}} > \omega_{\mathrm{MI}}$. The relationship between two ionization rates $n_{e\text{-ini}}\omega_{\mathrm{CI}}$ and $N\omega_{\mathrm{MI}}$ cannot be determined here.

Actually, the MI process becomes significant when $I > 10^{10}$ W/cm^2. Nevertheless, the CI only occurs with enough "seed electrons." Whether the free electrons in gas are sufficient to serve as the "seed electrons" depends on the focal spot volume of the laser beam V_F and the free electron density n_e[26]. If $n_e V_F^{-1} < 1$, there is barely one electron in the focal volume of the laser pulse and CI is not able to take place due to the absence of "seed electrons." Thus, it is only if $n_e V_F^{-1} > 1$ same as $n_e > V_F^{-1}$ that the CI process would be initiated[13,20].

When a Gaussian beam is focused by a quartz lens, the focal volume can be expressed as $V_F = \pi \int_{-z_R}^{z_R} \omega_s^2(z)\mathrm{d}z$, where $\omega_s(z) = \omega_0(1 + \frac{z^2}{z_R^2})^{\frac{1}{2}}$. The domain of the integration

runs through the entire focal depth $2Z_R = \frac{2\pi\omega_0^2}{\lambda}$ which doubles the Rayleigh length Z_R[20]. The ω_0 represents the radius of the focal spot, which can be obtained by the Gaussian focus equation $\omega_0 = \frac{\lambda f}{\pi\omega_p}$, where λ is the wavelength, f is the focal length of the quartz lens, and ω_P is the radius of the original laser beam. In our experimental condition, $\omega_P = 0.25$ cm and $f = 0.65$ cm, so the focal volume can be obtained to be $V_F = 1.48 \times 10^{-7}$ cm^{-3}. Thus, $n_{e\text{-ini}} \ll V_F^{-1} = 6.73 \times 10^6$ cm^{-3}, and the CI process would be absent at first. In this case, the MI process takes place first and provides the free electrons until the critical condition $n_e \approx V_F^{-1}$ is fulfilled[18–20]. Then, the CI process takes place.

Thus, it is reasonable to make an assumption that the laser-induced breakdown in atmospheric air takes place in two steps:

(1) The MI step produces the sufficient number of initial electrons for CI until the criterion n_{e0} is attained;
(2) Then, the CI-dominated step occurs.

In theory, the non-linear ionization equation group for atmospheric air can be expressed as follows, since the air is made up of nitrogen and oxygen with the ratio of about 8∶2:

$$\frac{\mathrm{d}n_e}{\mathrm{d}t} = \frac{NA_{\mathrm{N}_2}}{k_{\mathrm{N}_2}^{3/2}} I^{k_{\mathrm{N}_2}}(t) \times 0.8 + \frac{NA_{\mathrm{O}_2}}{k_{\mathrm{O}_2}^{3/2}} I^{k_{\mathrm{O}_2}}(t) \times 0.2, \tag{2}$$

$$\frac{\mathrm{d}n_e}{\mathrm{d}t} = n_e N\left[\frac{377q}{\omega^2}\left(\frac{v_{m\mathrm{N}_2}}{N}\right)^2\right] I(t) \times 0.8 + n_e N\left[\frac{377q}{\omega^2}\left(\frac{v_{m\mathrm{O}_2}}{N}\right)^2\right] I(t) \times 0.2. \tag{3}$$

Equation (2) elucidates the process of MI, where $\mathrm{d}n_e/\mathrm{d}t$ is the changing rate of free electrons in the focal position. k_{N_2} and k_{O_2} are the minimum number of laser photons for MI of N_2 and O_2, and A_{O_2} and A_{N_2} are the transition probabilities of O_2 and N_2, respectively. The latter one describes the process of CI. For atmospheric air, $q \approx 4.29 \times 10^{20}$, $V_{m\mathrm{O}_2} = 4.4 \times 10^9$ Ps^{-1} Torr, and $V_{m\mathrm{N}_2} = 5.5 \times 10^9$ Ps^{-1} Torr[10].

The spatial pulse length can be represented as $c\tau$, where c represents the light velocity and τ represents the pulse duration, and the size of the focal region can be represented as $2Z_R$. The parameter $N_Z = \frac{l_p}{z_R} = \frac{c\tau}{z_R}$ is used to characterize the ratio of the pulse length to the focal region (Rayleigh range). In our experiment, the value is much larger than one, which implies that the laser pulse is much larger than the focal region, so the laser intensity in the focal area can be considered to be uniform[30]. Therefore, the laser intensity is only the function of time in the focal region. $I(t)$ can be expressed as[31]

$$I(t) = I_{\mathrm{MAX}} \exp\left[(-4\ln 2)\left(\frac{t}{\tau}\right)^2\right], \tag{4}$$

where $I_{\max}$ is the peak power intensity, τ is the width of a pulse, and t is the propagation time for a laser pulse in the focal spot. The laser intensity peak arrives at the center of the focal region at $t = 0$.

So the ionization equations can be represented in two steps, as follows:

(1). MI step:

$$\frac{\mathrm{d}n_e}{\mathrm{d}t} = \frac{NA_{\mathrm{N}_2}}{k_{N_2}^{3/2}} I_{\mathrm{MAX}}^{k_{\mathrm{N}_2}} \exp\left[(-4k_{\mathrm{N2}}\ln 2)\left(\frac{t}{\tau}\right)^2\right] \times 0.8 + \frac{NA_{\mathrm{O}_2}}{k_{\mathrm{O}_2}^{3/2}} I_{\mathrm{MAX}}^{k_{\mathrm{O}_2}} \exp\left[(-4k_{\mathrm{O2}}\ln 2)\left(\frac{t}{\tau}\right)^2\right] \times 0.2. \tag{5}$$

We assume that the first step begins as soon as the pulse arrives at the focal region and the electron density reaches up to $n_{e0} = 6.73 \times 10^6$ cm^{-3} at the time of t_0, which is the time node separating step 1 and step 2. After integration, the formula above can be expressed as

$$n_{e0} = \frac{NA_{\mathrm{N}_2}}{k_{\mathrm{N}_2}^{3/2}} I_{\mathrm{MAX}}^{k_{\mathrm{N}_2}} \int_{-\infty}^{t_0} \exp\left[(-4k_{\mathrm{N}_2}\ln 2)\left(\frac{t}{\tau}\right)^2\right] \times 0.8\mathrm{d}t + \frac{NA_{\mathrm{O}_2}}{k_{\mathrm{O}_2}^{3/2}} I_{\mathrm{MAX}}^{k_{\mathrm{O}_2}} \int_{-\infty}^{t_0} \exp\left[(-4k_{\mathrm{O}_2}\ln 2)\left(\frac{t}{\tau}\right)^2\right] \times 0.2\mathrm{d}t, \tag{6}$$

where $k_{\mathrm{N}_2} = 13$ for nitrogen and $k_{\mathrm{O}_2} = 11$ for oxygen when the laser wavelength is 1064 nm. The threshold of the laser-induced breakdown in air is in the order of 10^{12} to 10^{13} W/cm^2, if we assume that the threshold is approximately 10^{12} W/cm^2 and substitute it into Eq. (6). It is found that the first term is 5 to 8 orders of magnitude smaller than the second term, so it can be ignored. Thus, the formula can be simplified into

$$n_{e0} = \frac{NA_{\mathrm{O}_2}}{k_{\mathrm{O}_2}^{3/2}} I_{\mathrm{MAX}}^{k_{\mathrm{O}_2}} \int_{-\infty}^{t_0} \exp\left[(-4k_{\mathrm{O}_2}\ln 2)\left(\frac{t}{\tau}\right)^2\right] \times 0.2\mathrm{d}t, \tag{7}$$

where $n_{e0} = 6.73 \times 10^7$ cm^{-3}.

(2). CI-dominated step:

When the density of initial electrons gets to $n_{e0} = 6.73 \times 10^6$ cm^{-3} by the MI step, CI occurs. In this step, although MI continues, the production of free electrons by MI can be negligible compared to the CI process. So only the CI process, which dominates this step, is considered. CI can be represented by a differential equation with separable variables when a new parameter such as $\alpha = N\left(\frac{377q}{\omega^2}\left(\frac{v_{m\mathrm{N}_2}}{N}\right)^2\right) \times 0.8 + N\left(\frac{377q}{\omega^2}\left(\frac{v_{m\mathrm{O}_2}}{N}\right)^2\right) \times 0.2$ is introduced. Then, Eq. (3) is transformed into:

$$\frac{\mathrm{d}n_e}{\mathrm{d}t} = n_e \alpha I_{\mathrm{MAX}} \exp\left[(-4\ln 2)\left(\frac{t}{\tau}\right)^2\right]. \tag{8}$$

This step starts at the time of t_0. After integration from t_0 to $+\infty$, the equation becomes:

$$n_{e\text{-final}} = n_{e0} \exp\left\{\alpha I_{\text{MAX}} \int_{t_0}^{+\infty} \exp\left[(-4 \ln 2)\left(\frac{t}{\tau}\right)^2\right] \mathrm{d}t\right\}. \quad (9)$$

The breakdown is defined as the fractional ionization of gas atoms in the focal region[9,10,32] or when the density of the final electron density $n_{e\text{-final}}$ reaches $n_{e\text{-th}} = 10^{16}$ cm^{-3}[9,18,33–35]. The density of the particles in atmospheric air is $N = 2.68 \times 10^{19}$ cm^{-3}[20]. So we know that the breakdown criterion of air is about $n_{e0} = \delta N = 2.68 \times 10^{16}$ cm^{-3}. When both Eqs. (7) and (9) are satisfied, the breakdown happens.

The threshold can be evaluated by working through a set of differential equations composed of Eqs. (7) and (9). We first give a tentative value to t_0 and plug it into Eqs. (7) and (9), respectively. Then, the solutions of the two equations for the several tentative values of t_0 can be obtained. Taking the situation with 1 atm pressure shown in Fig. 1 as an example, I_{MAX1} is the solution for the first differential equation and I_{MAX2} is the solution for the second one. When $I_{\text{MAX1}} = I_{\text{MAX2}}$, the value of t_0 is appropriate because the values of t_0 and I_{MAX} (where $I_{\text{MAX}} = I_{\text{MAX1}} = I_{\text{MAX2}}$) can satisfy the two equations at the same time.

Now the results from the experiments and two-step model will be compared and discussed. The breakdown threshold values obtained from the experiment at an atmospheric pressure are shown in Fig. 2. It is observed that the experimental threshold of each time fluctuates slightly, but is always near an average value of 1.29×10^{12} W/cm^2, so the threshold can be taken as 1.29×10^{12} W/cm^2. The fluctuation is attributed to observation errors and the fluctuation of the laser intensity, but is within reasonable bounds.

The experimental thresholds for air breakdowns at different pressures are in Fig. 3. The theoretical results are illustrated in Fig. 3 as well. For atmospheric pressure, the threshold of laser-induced breakdown is about 6.45×10^{12} W/cm^2 which is in good agreement with the result of our experiment.

For comparison, the theoretical simulation done the traditional way has been illustrated in Fig. 3 as well. The

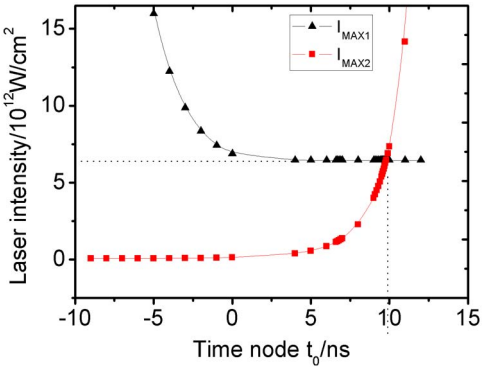

Fig. 1. The evolution of the values of I_{MAX1} (triangles) and I_{MAX2} (squares) with tentative time node t_0.

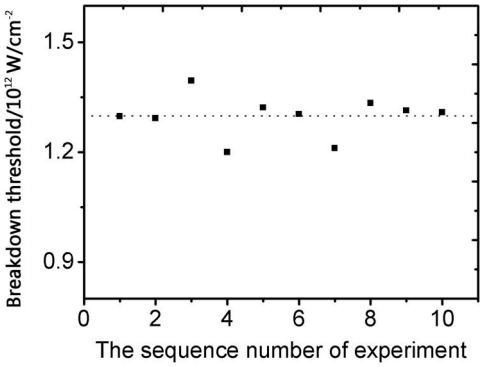

Fig. 2. Breakdown threshold obtained from experiments under atmospheric conditions.

results of the simulation of the two-step process fit the experimental data better within the whole pressure range. The results reveal the rationality of the present model. The advantage of this two-step model is more remarkable in low-pressure conditions. This is because when the pressure is low, the CI process is weaker at the beginning due to the insufficiency of the "seed electrons" in the rarefied air. The two-step ionization is more reasonable. When the pressure is very high (beyond 10^5 Torr), however, the initial density of the "seed electron" to initiate the CI process is achieved naturally in high-density air, and the CI process could start at the beginning of the laser pulse. The two-step model changes to the traditional ionization model. This is why the experimental results beyond 10^5 Torr deviate from our model and approach those of the traditional one.

That the calculated threshold is a bit larger than the measurement at a relatively high pressure may be attributed to penning ionization. Impurities with large ionic potentials in air, which can be excited by the laser pulse, collide with other air molecules and lead to a decrease of the breakdown threshold.

According to the theory of the non-linear interaction between nanosecond laser pulse and air, we divide the laser-induced breakdown into two steps based on the

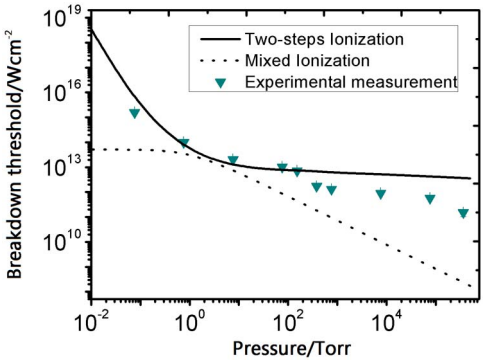

Fig. 3. Dependence of breakdown threshold obtained on air pressure. (a) Simulation results for two-step ionization model (solid line). (b) Simulation results for traditional model (dotted line). (c) Experimental results (triangles).

Morgan model: the MI, and CI-dominated step. The former provides the initial electrons for the CI process until the electron density reaches $n_{e0} = 6.73 \times 10^6$ cm^{-3} under the present experimental conditions. The latter is dominated by the CI. The numerical calculation of the breakdown threshold agrees with the experimental value in a large pressure range (up to 10^5 Torr), which shows the rationality of the two-step ionization model. Furthermore, the time node dividing the two steps is obtained as 9.8 ns at atmospheric pressure. The model of the two-step ionization proposed here is essential for understanding the whole laser-induced air breakdown process.

This work was financially supported by the National Natural Science Foundation of China under Grant Nos. 11274204 and 11474187.

References

1. R. G. Meyerand, Jr. and A. F. Haught, Phys. Rev. Lett. **11**, 401 (1963).
2. J. Zhao, Chin. Opt. Lett. **12**, 083201 (2014).
3. Y. Y. Zhang, C. S. Chen, X. L. Zhou, J. Guo, Q. G. Zhang, and B. Y. Man, Chin. Opt. Lett. **4**, 080493 (2006).
4. J. Y. Mo, Y. Q. Chen, R. H. Li, Q. Zhou, and Y. Lou, Chin. Opt. Lett. **12**, 083001 (2014).
5. C. L. Xie, J. D. Lu, P. Y. Li, J. Li, and Z. X. Lin, Chin. Opt. Lett. **7**, 060545 (2009).
6. J. Zhao, L. L. Zhang, Y. M. Luo, T. Wu, C. L. Zhang, and Y. J. Zhao, Chin. Opt. Lett. **5**, 010058 (2007).
7. P. Lu, L. S. Wang, H. Y. Hu, Z. Zhuang, Y. B. Wang, R. J. Wang, and L. T. Song, Chin. Opt. Lett. **11**, 053004 (2013).
8. H. Yashiro, F. Sasaki, and H. Furutani, Opt. Commun. **284**, 3004 (2011).
9. C. G. Morgan, Prog. Phys. **38**, 621 (1975).
10. Y. E. Gamal and M. A. Harith, J. Phys. D: Appl. Phys. **14**, 2209 (1981).
11. C. L. M. Ireland and C. G. Morgan, J. Phys. D: Appl. Phys. **6**, 720 (1973).
12. L. V. Keldysh, Sov. Phys. JETP **20**, 1307 (1965).
13. E. W. Van Stryland, M. J. Soileau, A. L. Smirl, and W. E. Williams, Phys. Rev. B **23**, 2144 (1981).
14. L. Wang, C. J. Zhang, and Y. Feng, Opt. Lett. **06**, 5 (2008).
15. N. Korll and K. M. Watson, Phys. Rev. A **5**, 1883 (1972).
16. D. C. Smith and M. C. Fowler, Appl. Phys. Lett. **22**, 500 (1973).
17. D. C. Smith, Appl. Phys. Lett. **19**, 405 (1971).
18. D. I. Rosen and G. Weyl, J. Phys. D: Appl. Phys. **20**, 1264 (1987).
19. A. Musing, U. Riedel, J. Warnatz, W. Herden, and H. Ridderbusch, Proc. Combust Inst. **31**, 3007 (2007).
20. J. H. Han, G. Y. Feng, L. M. Yang, and Q. H. Zhang, Acta. Phys. Sinica **57**, 6304 (2008).
21. C. S. Chen, B. Y. Man, X. Song, D. Liu, and H. B. Fu, Phys. Plasmas **19**, 043501 (2012).
22. H. B. Fu, C. S. Chen, B. Y. Man, X. Song, and D. Liu, Eur. Phys. J. D **65**, 509 (2011).
23. H. B. Fu, C. S. Chen, B. Y. Man, X. Song, and D. Liu, Phys. Plasmas **19**, 032303 (2012).
24. C. S. Chen, A. H. Liu, G. Sun, J. L. He, X. Q. Wei, M. Liu, Z. G. Zhang, and B. Y. Man, J. Opt. A: Pure Appl. Opt. **8**, 88 (2006).
25. T. X. Phuoc, Opt. Commun. **175**, 419 (2000).
26. G. H. Canavan and P. E. Nielsen, Appl. Phys. Lett. **22**, 409 (1973).
27. X. M. Zhao, J. C. Diels, C. Y Wang, and J. M. Elizondo, Quant. Electron. IEEE J. **31**, 599 (1995).
28. E. G. Gamaly, A. V. Rode, V. T. Tikhonchuk, and B. Luther-Davies, Appl. Surf. Sci. **197–198**, 699 (2002).
29. O. A. Louchev, P. Bakule, N. Saito, S. Wada, K. Yokoyama, K. Ishida, and M. Iwasaki, Phys. Rev. A **84**, 033842 (2011).
30. P. K. Kennedy, D. X. Hammer, and B. A. Rockwell, Quant. Electr. **21**, 155 (1997).
31. C. H. Fan and J. P. Longtin, Appl. Opt. **40**, 3124 (2001).
32. Y. E. E. D. Gamal and I. M. Azzouz, J. Phys. D Appl. Phys. **34**, 3234 (2001).
33. B. C. Stuart, M. D. Feit, S. Herman, A. M. Rubenchik, B. W. Shore, and M. D. Perry, Phys. Rev. B **53**, 1749 (1996).
34. J. Hermann and T. L. Floch, J. Appl. Phys. **96**, 3084 (2004).
35. A. Sircar, R. K. Dwivedi, and R. K. Thareja, Appl. Phys. B **63**, 623 (1996).